Artvin Çoruh Üniversitesi
Doğal Afetler Uygulama ve Araştırma Merkezi
Doğal Afetler ve Çevre Dergisi

Artvin Çoruh University
Natural Hazards Application and Research Center
Journal of Natural Hazards and Environment

Araştırma Makalesi / Research Article, Doğ Afet Çev Derg, 2026; 12(1): 159–168, DOI: 10.21324/dacd.1764600

Evaluation of Simulated Rainfall Patterns in Control Plot Subsections

Abdullah Emin Demircioğlu[1,*], Erdal Kesgin[2], Kadir Gezici[2,3], Selim Şengül[3], R. İlayda Tan Kesgin[4]

[1]*Marmara Üniversitesi, Mühendislik Fakültesi, İnşaat Mühendisliği Bölümü, 34722, İstanbul.*
[2]*İstanbul Teknik Üniversitesi, İnşaat Fakültesi, İnşaat Mühendisliği Bölümü, 34469 İstanbul.*
[3]*Atatürk Üniversitesi, Mühendislik Fakültesi, İnşaat Mühendisliği Bölümü, 25100, Erzurum.*
[4]*Fatih Sultan Mehmet Vakıf Üniversitesi, Mühendislik Fakültesi, İnşaat Mühendsiliği Bölümü, 34445, İstanbul.*

Abstract

Rainfall simulators have been used for many years in laboratory settings to simulate natural rainfall. This natural precipitation produced in a laboratory environment is particularly important for hydrological research in controlled laboratory environments where its natural variability can be examined in detail. This study examines the spatial variability of rainfall's fundamental parameters, intensity, uniformity, and drop diameter, in a nine-subarea arrangement within a single-channel rainfall simulator. To observe how the distribution patterns change depending on rainfall intensity within the simulator's operating range of 30-140 mmh^{-1}, we conducted simulations at four different intensities (40, 70, 80, and 100 mmh^{-1}). Within the channel area, I (rainfall intensity) showed local variations. Similarly, Christiansen's uniformity coefficients (CU) ranged from 69% to 95%. However, local CU values in some sub-regions were significantly lower than these averages. D_{50} (median drop diameter) varied between 1.32 and 1.77 mm for different densities and sub-areas. Generally, it was observed that homogeneity improved as rainfall intensity increased, but there were still significant differences within the area. The size of the raindrops varies depending on where they fall, with larger drops generally observed in the middle of the area (A3, A4, A5). These results contradict the common assumption of uniform rainfall intensity within the channel area and highlight the necessity of sub-area-based analysis for the accurate interpretation of simulated rainfall experiments.

Keywords
Rainfall Simulator, Christiansen Uniformity, Drop-Size Distribution, Spatial Variability, Sub-Area Analysis

Simüle Edilmiş Yağış Desenlerinin Ölçüm Alt Alanlarında Değerlendirilmesi

Özet

Yağış simülatörleri laboratuvar ortamlarında doğal yağışı simüle etmek için uzun yıllardır kullanılan cihazlardır. Bu laboratuvar ortamında üretilen doğal yağışın özellikle doğal değişkenliği ayrıntılı olarak incelenebildiği kontrollü laboratuvar ortamlarında, hidrolojik araştırmalar için önemli olmaktadır. Bu çalışma, bir kanallı yağış simülatörü içinde dokuz alt alana ayrılmış bir düzende yağışın temel parametreleri olan şiddet, düzgünlük ve damla çapının mekânsal değişkenliğini incelemektedir. Simülatörün 30-140 mmh^{-1}'lik çalışma aralığında, yağış şiddetine bağlı olarak dağılım desenlerinin nasıl değiştiğini görmek amacıyla dört farklı yoğunlukta (40, 70, 80 ve 100 mmh^{-1}) simülasyonlar gerçekleştirdik. Kanal alanı içerisinde I (yağış şiddeti) lokal olarak farklılıklar göstermiştir. Aynı şekilde Christiansen uniformluk katsayılarıda (CU) %69 ile %95 arasında değişmiştir. Fakat bazı alt bölgelerdeki lokal CU değerleri bu ortalamaların çok daha altında kalmıştır. D_{50} (medyan damla çapı), farklı yoğunluklar ve alt alanlarda 1,32 ile 1,77 mm arasında değişiklik göstermiştir. Genel olarak, yağış şiddeti arttıkça homojenlik iyileştiği fakat alan içinde hala önemli farklılıklar olduğu gözlemlenmiştir. Yağmur damlalarının boyutu düştükleri yere göre değişmektedir; genellikle alanın ortasında daha büyük damlalar gözlemlendi (A3, A4, A5). Bu sonuçlar, kanal alanı içinde aynı şiddette ve tekdüze bir yağış olduğu şeklindeki yaygın varsayımıyla çelişmekte ve simüle edilmiş yağış deneylerinin doğru şekilde yorumlanması için alt alan bazlı analizin gerekliliğini vurgulamaktadır.

Anahtar Sözcükler
Yağmur Simülatörü, Christiansen Uniformluk Katsayısı, Damla Boyut Dağılımı, Mekânsal Değişkenlik, Alt-Bölge Analizi

1. Introduction

Rainfall simulators (RS) have been used for many years as an important tool in laboratory settings for a wide variety of agricultural, urbanization, hydrological, and geomorphological experiments, such as drainage, seepage, rainfall-runoff processes, land management-rehabilitation, and erosion (Abudi et al., 2012; Zhang et al., 2014; Kesgin et al., 2020a; Gezici et al., 2021).

*Sorumlu Yazar: Tel: +90 (216) 7773799 Faks: +90 (216) 7770001
E-posta: emin.demircioglu@marmara.edu.tr (Demircioğlu A.E.)
kesginerdal@gmail.com (Kesgin E.), kadirgezici@atauni.edu.tr (Gezici K.)
ssengul@atauni.edu.tr (Şengül S.), ritankesgin@fsm.edu.tr (Tan Kesgin R.I.)

Gönderim Tarihi / Received : 13/08/2025
Kabul Tarihi / Accepted : 11/01/2026

The most important advantages of these simulators are (1) having control over the intensity, duration, and most importantly, the repeatability of rainfall (no need to wait for natural rainfall), and (2) being able to isolate environmental factors (temperature, wind, humidity etc.) being affected or managing these factors (Mhaske et al., 2019). These advantages lead to reduced research costs and shortened study durations.

However, the ability of RS in replicating the characteristics of natural rainfall (rainfall intensity, spatial uniformity, raindrop diameter, terminal velocity, and kinetic energy) is a critical concern (Abdollahi, 2011). It is desired that the simulator consistently reproduces these variables within certain standards (Kathiravelu et al., 2016). Simulators that can accurately mimic natural precipitation patterns can recreate real-world rain events with specific intensities and durations, facilitating in-depth studies of processes including infiltration, drainage, erosion, land management and rehabilitation, rainfall-runoff, and irrigation (Kesgin et al., 2018; Kesgin et al., 2023). Gezici et al. (2025) emphasized that this situation makes RS an effective tool in water management and solving rainfall-related environmental problems.

While these simulators have many benefits, they also have some disadvantages and limitations. These limitations include (1) producing high-intensity rainfall (even when system pressure is at a minimum), (2) the lack of standardized design and calibration processes for critical features such as system pressure, simulator height, parcel sizes, and the number and position of nozzles, (3) inability to characterize complex and large-scale basins due to small-scale system installations and (4) the representation of key parameters affecting natural rainfall (rainfall intensity, spatial uniformity, raindrop diameter) with single values regardless of channel dimensions, and their failure to capture some local differences in percentage (Pérez-Latorre et al., 2010; Gezici et al., 2025).

The parameters used for precipitation studies (rainfall intensity, uniformity, and raindrop diameter) are often considered as average values for the entire study area (Gezici et al., 2021; Koch et al., 2024). When local differences are not taken into account, similar uniform input assumptions can also lead to bad results in hydraulic and data-based models for water networks, river flow, rainwater harvesting, and rain gardens (Saplıoğlu & Küçükerdem, 2018; Küçükerdem et al., 2019; Saplıoğlu et al., 2019; Şenel et al., 2020; Koşucu et al., 2021; Saplıoğlu & Küçükerdem Öztürk, 2024; Küçükerdem Öztürk et al., 2025; Tan Kesgin, 2025). But this assumption doesn't mean that all parts of the area get rain in the same way or that the effects are completely the same. Researchers often treat the key parameters used in rainfall simulator studies -rainfall intensity, spatial uniformity, and raindrop-size distribution- as single average values for the whole plot (Gezici et al., 2021). This general assumption does not mean that the same amount of rain falls evenly over all parts of the land or that the way water reacts is the same everywhere. In practice, local variations in rainfall intensity, *CU,* and drop-size distribution can substantially modify infiltration, runoff generation, and erosion rates. Assuming a spatially uniform rainfall field may therefore mask important intra-plot gradients and lead to biased interpretations of experimental results. To achieve more realistic and reliable results, it is crucial to examine the spatial distribution of rainfall parameters. However, several rainfall-simulator studies have clearly divided the plot into multiple sub-areas and evaluated the co-variation of spatial gradients in *I*, *CU*, and drop-size distribution in a single control plot (Green & Pattison, 2022; Ma et al., 2023; Luza et al., 2024; Rončević et al., 2025).

Recent studies on RS have increasingly focused on parcel-scale spatial rainfall patterns, Christiansen uniformity (*CU*), and drop size distribution, as well as how closely laboratory and field devices reproduce the characteristics of natural rainfall. Green and Pattison (2022) have shown that intensive cover use can reveal some significant local variability that is missed in coarser arrangements. Other authors have developed portable or highly optimized sprinkler systems that better reproduce natural drop size spectra and kinetic energy (Fernández-Raga et al., 2022; Lasisi et al., 2022; Rončević et al., 2025).

Building on these studies our research, a flume-type rainfall simulator divided into nine smaller areas is used to examine the distribution of *I* (rainfall intensity), the *CU* (Christiansen uniformity) coefficient, and the D_{50} (median drop diameter). We did this using two different basin configurations (Pattern-1 and Pattern-2) and four different rainfall intensity (40, 70, 80, and 100 mmh^{-1}) levels. This study looks closely at how *I*, *CU*, and D_{50} change across a plot by using a dense sampling grid and dividing the plot into three parts: upstream, central, and downstream. It also looks at how these things change together on the control plot. The study enhances prior initiatives aimed at calibrating rainfall simulators centered on plot-average performance metrics.

2. Materials and Methods

2.1. Design of the Rainfall Simulator

The experiments were conducted using the existing RS at the Hydraulics Laboratory of Istanbul Technical University. The system includes a rainfall channel that is 2.7 meters long and 1.20 meters wide (Figure 1a-b). Four Fulljet B1/GG-12W nozzles (Spraying Systems), positioned at intervals as shown in Figure 2, are mounted 2.40 meters above the channel base. These nozzle types provide a conical spray at an angle of 120°, ensuring uniform and standard-compliant rainfall distribution. Tap water is drawn from a 500-liter tank using a pump and delivered to the nozzles through PVC pipe. This study utilized a stationary, pressurized-driven rainfall simulator featuring full-cone nozzles, powered by a pump. This design is similar to other pressurized laboratory simulators that try to make the environment the same while also trying to copy the natural drop-size spectra and kinetic energy (Fernández-Raga et al., 2022; Lasisi et al., 2022; Rončević et al.,

2025). Four different rainfall intensities, designated as R1, R2, R3, and R4, were used to evaluate the similarity of laboratory-generated rainfall to natural rainfall. These intensities were set at 40, 70, 80, and 100 mmh^{-1}. Rainfall intensity was calculated using Equation 1, formulated by Sousa et al. (2017) to measure rainfall intensity produced by the system operating at a specific flowrate. To make sure the results could be repeated, each intensity-pattern combination was done three times. This cut down on random variability in the measurements.

$$I_r = \left(\frac{V}{St}\right) 60 \tag{1}$$

Where I_r rainfall intensity (mmh^{-1}), V the amount of water gathered in the containers (L), S representing the surface area of the containers (m^2), and t indicating the rainfall duration (min)

2.2. Rainfall Uniformity

The spatial uniformity of simulated rainfall was determined using the Christiansen Uniformity Coefficient (CU, %) proposed by Christiansen (1941) (Equation 2). According to Mhaske et al. (2019), a CU value close to 80% is considered reasonable, while Luk et al. (1993) suggested that this threshold could be reduced to 70% for larger field areas.

$$CU = 100\left(1 - \frac{\sum_{i=1}^{N} |x_i - \bar{x}|}{n\bar{x}}\right) \tag{2}$$

Where x_i its means the quantity of water in each container; i^{th} container, $\bar{x}$ shows the average amount collected from all the containers, and n shows how many containers were used to make the measurement.

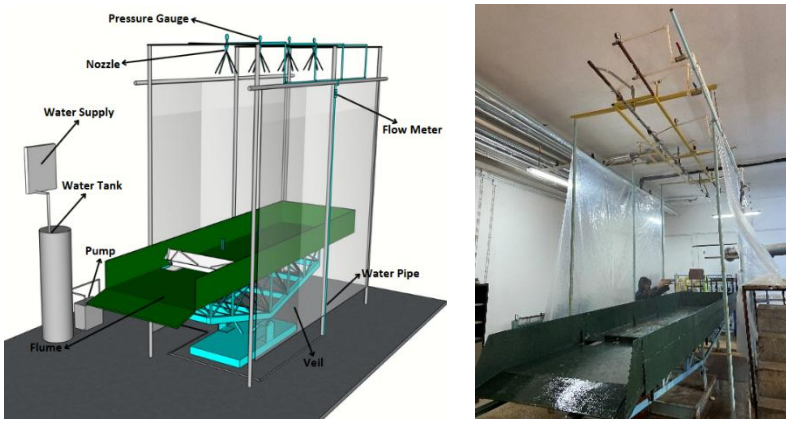

a) b)

Figure 1: a) 3D model of the rainfall simulator; b) Image of the experimental configuration in laboratory

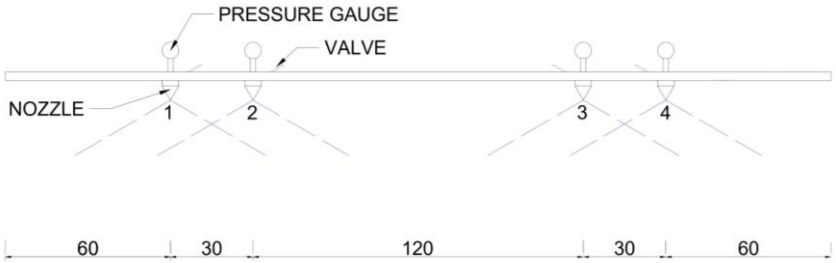

Figure 2: Nozzle positioning

2.3. Raindrop Diameter

There are many methods in the literature for determining the diameter of raindrops, among which the ones commonly used are the flour pellet method, radar reflectivity, optical dendrometers, and the stain method (Van Dijk et al., 2002; Kesgin et al., 2020b). The Flour Pellet Method is often the most popular of these methods because it is cheap and easy to repeat compared to other methods. Bentley (1904) first introduced this method. It has shown consistent reliability through widespread calibration efforts in hydrological studies (Clarke & Walsh, 2007; Moazed et al., 2010; Kesgin et al., 2018).

To do this, a tray is filled with a 2-centimeter-thick layer of flour and then covered with a lid. When the simulated rain intensity reaches the desired level, the lid is taken off so that the tray can be exposed to real rain for a few seconds. This lets the rain make small droplets in the flour layer. After this exposure, the tray is put in an oven at 105 °*C* for 24 hours to harden the pellets that formed when the raindrops hit. Kesgin et al. (2018) explain how to use sieve analysis to sort the hardened pellets and make granulometric curves. Subsequently, the median drop diameter (D_{50}) is calculated. This process is conducted repeatedly under varying rainfall intensities to generate data pairs that illustrate the correlation between rainfall intensity and D_{50}.

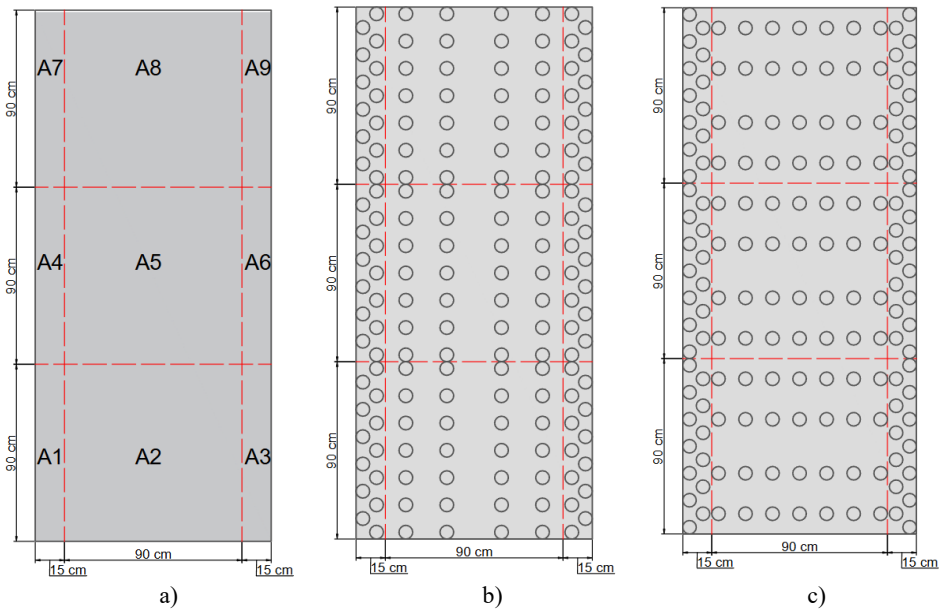

Figure 3: a) Subsections of the rainfall channel, b) Pattern-1, c) Pattern-2

Figure 3 presents a detailed schematic showing the division of the channel into lower compartments and the cup arrangements used in these compartments. Because the edge areas are smaller, Pattern 1 and 2 have cup arrangements that are more diagonal and frequent, as seen in Figures 3b-c. Pattern 1 (Figure 3b) was used to observe vertical variations in the middle sections of the channel, while Pattern 2 (Figure 3c) was used to observe horizontal changes. In the group evaluation of sub-areas, A1-A2-A3 were considered upstream, A4-A5-A6 were considered central, and A7-A8-A9 were considered downstream. The experiment was conducted in a manner supported by research studies that show the installation pattern configuration and nozzle spacing greatly influence the overall fluid movement and the localized rainfall distribution (Green & Pattison, 2022; Henorman et al., 2022; Ma et al., 2023; Rončević et al., 2025).

3. Results and Discussion

3.1. Spatial variability of rainfall intensity (*I*)

The system was operated under four different rainfall intensities, R1 (40 mmh^{-1}), R2 (70 mmh^{-1}), R3 (80 mmh^{-1}), and R4 (100 mmh^{-1}), and in two different configurations (Pattern-1 and Pattern-2). Figure 4 shows how rainfall intensity changes spatially along the channel for different rainfall intensities and different arrangements. The distribution of rainfall intensity showed significant spatial variations within the channel. For example, during R1 rainfall (Figures 4a and 4b), rainfall intensity decreased spatially to 30 mmh^{-1} in some sub-regions, while it increased to 55 mmh^{-1} in other sub-regions (Table 1). However, when evaluated at a point scale, rainfall intensity decreased to 20 mmh^{-1} at specific points, particularly in the downstream of the channel, while it increased to 90 mmh^{-1} at some measurement points. Sub-section analyses showed that rainfall was more uniform in the middle sections of the channel, while significant fluctuations were observed in the upstream and downstream sections. Under R2 rainfall intensity (Figures 4c and 4d), the intensity varies between 25 and 125 mmh^{-1} at some measurement points and spatially between 47 and 99 mmh^{-1}, showing a more even distribution, especially in the middle section of the channel (Table 1). Measurements taken in the lower regions showed that this density level made the distribution more even along the channel.

At higher rainfall intensities, R3 and R4 (Figures 4e-h), while spatial differences persisted, the distribution within the channel became relatively balanced (Table 1). Under R4, the intensity of rainfall in the central parts of the channel was more evenly spread out around the average value, but the standard deviation between subareas was higher (Table 1). Subarea A1 usually had the highest rainfall intensity, while A3 always had the lowest values. Additionally, the amount of rainfall falling on the upstream and downstream sections of the channel is less than the amount falling on the middle

sections. As rainfall intensity increased, a general homogenization and a decrease in spatial variability were observed in the channel. Additionally, as rainfall intensity increased, the significant difference between A1 and A4 tended to decrease. In all experiments except for R1 rainfall intensity, A4 was calculated as the sub-region with the second-highest rainfall intensity. This indicates that A4 has a more significant impact on rainfall distribution, especially during periods of high rainfall intensity, and that rainfall is concentrated in this region.

The increased rainfall intensities in the middle regions of all scenarios are due to nozzle interference. To reduce the large changes caused by that interference, an extended gap was included in the nozzle configuration in the central part, thus increasing the gap between the nozzles. Past research upholds these findings. Green and Pattison (2022) and Demircioğlu et al. (2024) emphasized in their studies that regional differences in kinetic energy related to rainfall intensity and their effects on erosion are significant in other similar RS-requiring studies. Likewise, the research of Kesgin et al. (2017) revealed some spatial variation in the rainfall in drainage experiments. More recent research carried out by the works of Gezici et al. (2025) pointed to the spatial variability of the effects of rainfall uniformity. These experiments have been supported by the present research to a significant degree.

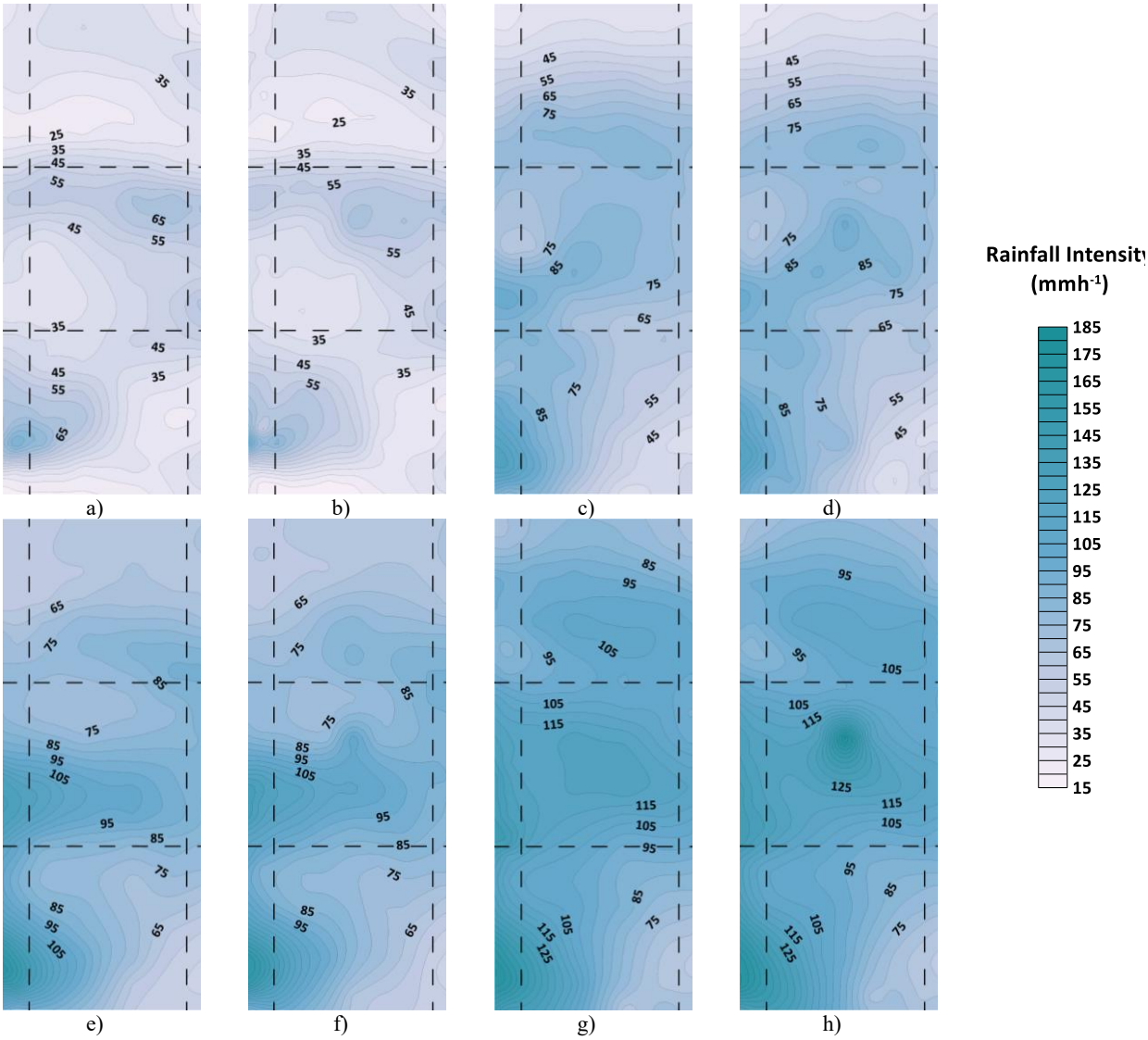

Figure 4: Rainfall Intensity Contour Maps: a) Pattern-1 and 40 mmh $^{-1}$, b) Pattern-2 and 40 mmh $^{-1}$, c) Pattern-1 and 70 mmh^{-1}, d) Pattern-2 and 70 mmh^{-1}, e) Pattern-1 and 80 mmh^{-1}, f) Pattern-2 and 80 mmh^{-1}, g) Pattern-1 and 100 mmh^{-1}, h) Pattern-2 and 100 mmh^{-1}

3.2. Spatial variability of Christiansen uniformity (*CU*)

In the system for the rainfall intensities R1, R2, R3, and R4, the uniformity coefficients (*CU*) obtained for the system from all the containers in the first setup reached a value of 74%, 76%, 80%, and 83%, respectively. The values obtained comply with both standards specified in section 2.2.

In the second setup of the experiment, the uniformity coefficients for the mentioned rainfall intensities reached a value of 73%, 76%, 80%, and 83%, respectively. In the preliminary experiment setup, the nozzle configuration shown in Figure 2 was determined to have the highest uniformity of rainfall in the channel. All the experiments therefore followed the nozzle configuration shown in Figure 2.

Figure 5 illustrates the uniformity distribution for rainfall intensities R1 to R4 under both configurations. For R1, the first configuration achieved an average uniformity coefficient of 74%, with local values ranging from 69% to 89% (Table 1). Subsection coefficients were 69%, 71%, 81%, 84%, 82%, 89%, 88%, 84%, and 83%. The second configuration had a slightly lower average uniformity of 73%, with local coefficients between 70% and 90% (Table 1). For R2, both configurations reached an average uniformity coefficient of 76%. Local variations were between 74% and 96% for the first configuration and from 69% to 95% for the second. The subsection coefficients are similar for both configurations. In both configurations, the uniformity increased with the increase in rainfall intensities. For R3, in both configurations the average uniformity was 80%, with a variation between 82% and 96% in both. Subsection coefficients are similar; however, higher uniformity was found in the central section's A4, A5, and A6. For R4, with the highest intensity of rainfall, the average uniformity coefficient reached 83% in both configurations. Local values varied between 81% and 93% in the first configuration and from 82% to 95% in the second one. Uniformity was lower at the channel's start (A1, A2, and A3) but improved significantly in central areas. Overall, uniformity increased with higher rainfall intensities, and both configurations produced comparable results, with the central section's consistently showing better uniformity.

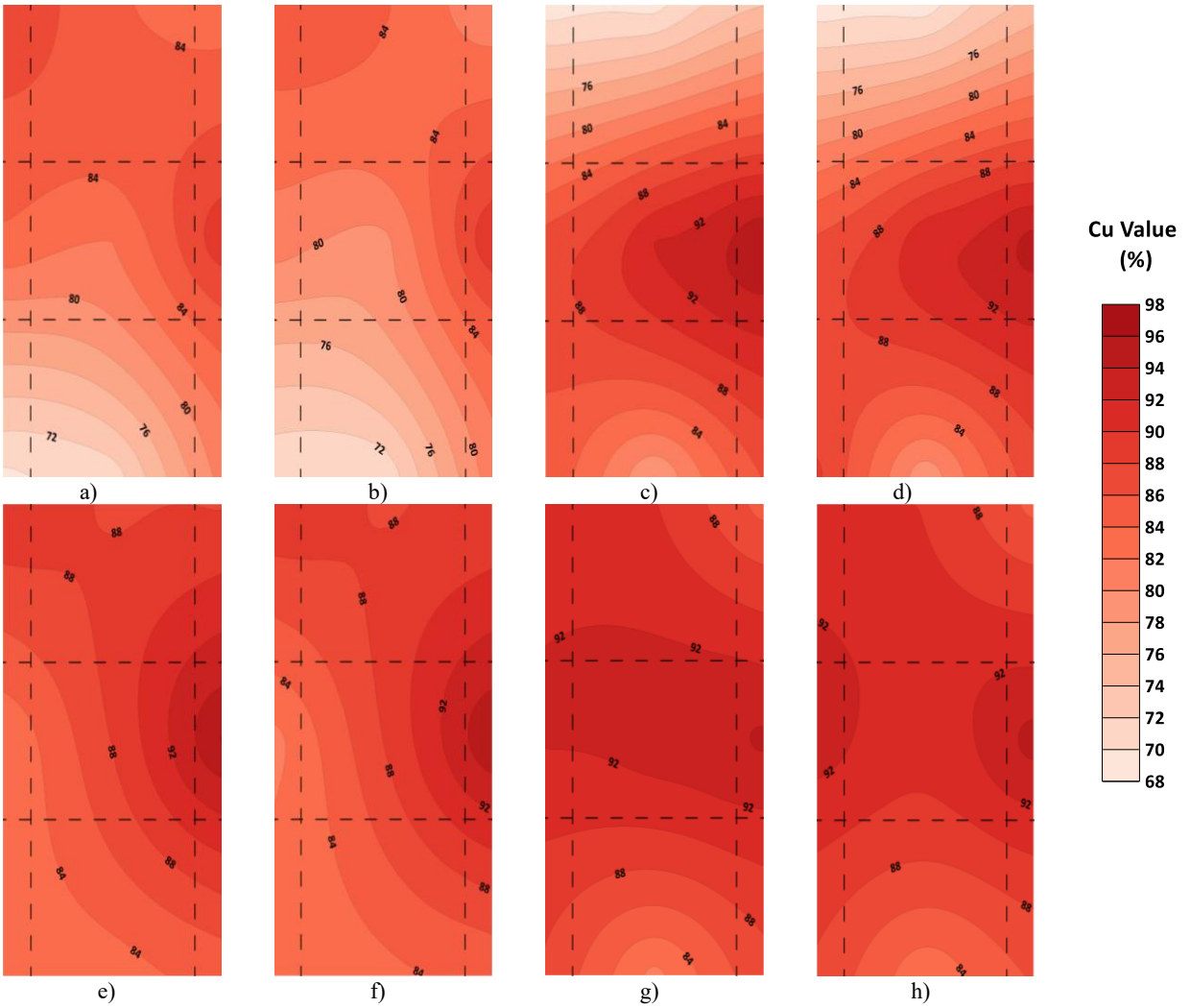

Figure 5: Contour maps of Uniformity (%): a) Pattern-1 and 40 mmh^{-1}, b) Pattern-2 and 40 mmh^{-1}, c) Pattern-1 and 70 mmh^{-1}, d) Pattern-2 and 70 mmh^{-1}, e) Pattern-1 and 80 mmh^{-1}, f) Pattern-2 and 80 mmh^{-1}, g) Pattern-1 and 100 mmh^{-1}, h) Pattern-2 100 mmh^{-1}

Generally, as the intensity of the rain increased, the uniformity of the rain also improved. This is clear from both the contour maps and the numbers. At lower intensities, the channel as a whole did not meet the standards that are usually used in the literature, but some areas did.

This highlights the need to analyze the uniformity of rainfall in the region instead of the whole (Gezici et al., 2025). Variations in the spatial regions offer a more in-depth analysis of the system. The study by Gezici et al. (2025) revealed the variation in the values of *CU* when different container setups were applied under the same conditions.

However, despite the different container arrangements in the results obtained from these experiments, the *CU* values showed similarities. This situation could stem from differences in sprayer types, channel dimensions, and collection containers. These discrepancies highlight the lack of an accepted standard for calibration and design processes in such systems (Kavian et al., 2018).

3.3. Spatial variability of drop-size distribution

Depending on the sub-area and precipitation levels, the calculated D_{50} (median diameters) values in this study varied from about 1.32 to 1.77 mm. According to previous laboratory rainfall experiments reported in the literature, this range is comparable to the natural distribution of moderate to high intensity rainfall (Fernández-Raga et al., 2022; Lasisi et al., 2022; Henorman et al., 2022; Ma et al., 2023; Rončević et al., 2025). The droplet size distributions are presented numerically in Table 1 and as spatial granulometric curves in Figure 6.

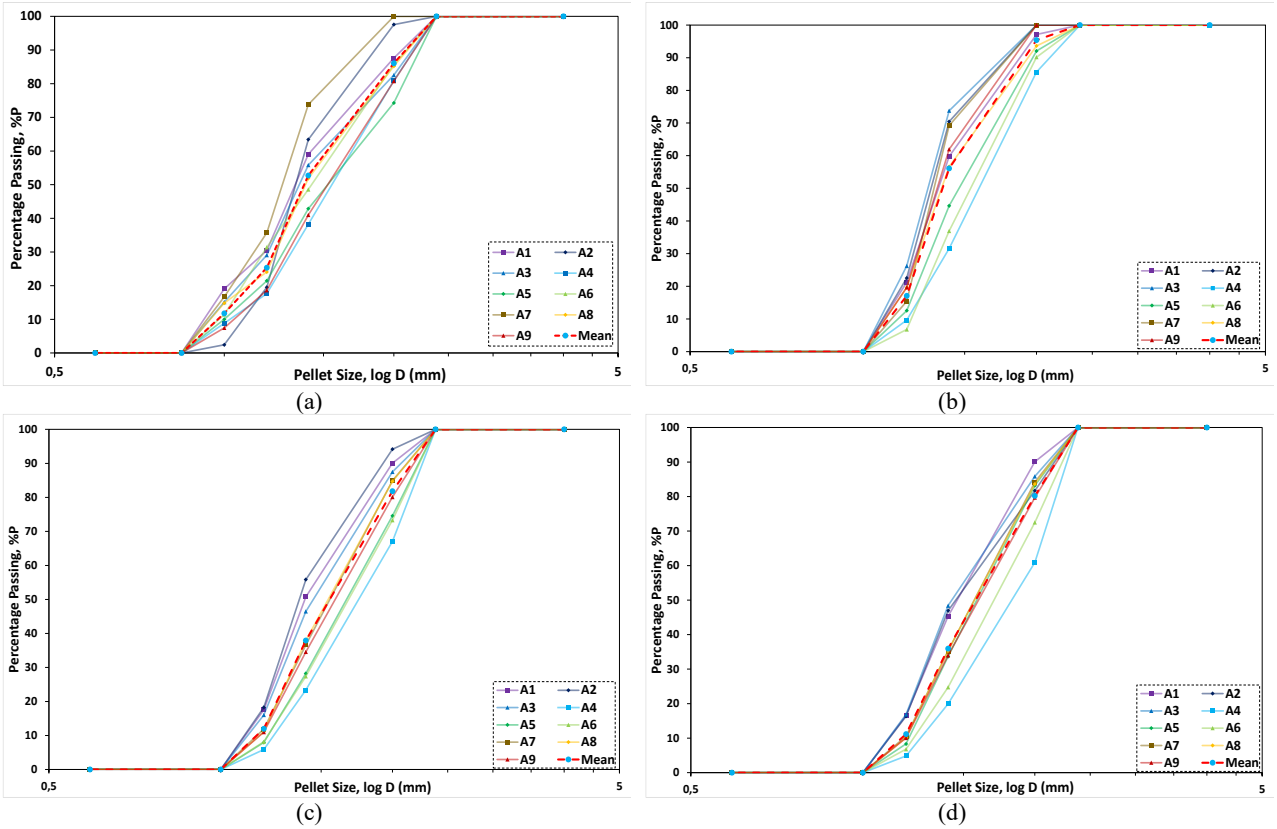

Figure 6: Pellet size distribution for different rainfalls: a) 40 mmh $^{-1}$, b) 70 mmh $^{-1}$, c) 80 mmh $^{-1}$, d) 100 mmh $^{-1}$

Table 1 presents the frequency density of the droplet size distribution and D50 values for each subregion and rainfall intensity. This depicts the variation in median drop size and drop size distribution across the upstream, central, and downstream regions of the plot. The table is useful because it relates the regional gradients at D50 to the changes that were observed in precipitation intensity and CU. The table provides a way of interpreting the particle size distribution curves shown in Figure 6. While studies by Confesor and Rodrigues (2018) and Iserloh et al. (2012) reported a decrease in droplet size with increasing system pressure, the opposite trend was observed in this study: droplet size increased with rising system pressure. Another notable observation is the regional variability in droplet sizes at the same rainfall intensity. An adequate rationale for the observed opposing trend is that, in our pressure-driven sprinkler system, increasing the intake pressure not only enhances discharge but also optimizes nozzle atomization and overlapping spray patterns. At intermediate pressures, the nozzle generates a diverse array of small to medium droplets. At elevated pressures, flow instabilities and jet coalescence might result in certain regions of the spray producing larger droplets (Fernández-Raga et al., 2022; Lasisi et al., 2022; Rončević et al., 2025). Also, the short distance between the nozzle and the surface and the small indoor space may reduce disintegration and evaporation during flight. That is, larger droplets made at high pressure can reach the plot surface without breaking, which is unlike other setups used by Confesor and Rodrigues (2018) and Iserloh et al. (2012).

Droplet sizes for the four rainfall intensities varied between 1.27 and 1.84 mm. For the lowest level of rain, R1, A7 had the smallest droplets, which were 1.27 mm in size, while A4, being in the middle of the channel, had the biggest droplets, having a size of 1.57 mm. Under the rainfall intensity with the lowest magnitude, R2, A3 had the smallest droplet size. Again, A4 had the largest droplet size. For R3, the sizes of the droplets ranged from 1.38 mm to 1.77 mm, with A2 having the smallest size and A4 having the largest size, which was the same as for other intensities. The smallest droplet size for R4 was 1.44 mm in the area with the least rain, and the largest droplet size was once again found in A4.

The results showed that the regions of smaller droplet size correlated to regions of lower rainfall intensity. But in the case of larger droplet sizes, the trend was not the same in all regions. Larger droplet sizes were visible in A4, the central region of the channel. In general, when there was an increase in the intensity of rainfall in some regions, there was no corresponding rise in larger droplet sizes. Instead, there was a decrease in the size of the droplets. There have been different techniques developed in the determination of droplet sizes.

These techniques have their own merits and demerits (Khaledian & Shahoe, 2007). According to Fornis et al. (2005), a larger sample size should be used to obtain a more precise droplet size in the flour pellet technique. The droplet sizes obtained in our research have been compared to the sizes in different research (Luk et al., 1993; Meshesha et al., 2013; Meshesha et al., 2016; Kesgin et al., 2018). The obtained droplet sizes fall in the range of droplet sizes determined by the range of Sousa et al. (2017), but the droplets obtained in our research are smaller since the sizes fall near the lower end of the range.

Table 1: Summary of the rainfall characteristics

Mean Rainfall Intensity (mmh^{-1})	Characteristics	Pattern	A1	A2	A3	A4	A5	A6	A7	A8	A9
R1	Intensity (mmh^{-1})	1	53	39	35	42	47	55	30	33	35
		2	53	39	36	42	47	54	30	33	36
	CU (%)	1	69	71	81	84	82	89	88	84	83
		2	70	70	81	81	79	90	86	84	80
	Drop diameter (mm)	Both	1.34	1.34	1.36	1.57	1.54	1.43	1.27	1.40	1.54
R2	Intensity (mmh^{-1})	1	98	66	47	79	76	70	51	57	54
		2	99	68	48	78	78	70	50	57	53
	CU (%)	1	86	78	86	87	92	96	69	69	74
		2	89	78	87	86	82	95	69	69	75
	Drop diameter (mm)	Both	1.35	1.32	1.30	1.61	1.48	1.55	1.33	1.37	1.35
R3	Intensity (mmh^{-1})	1	119	78	59	103	88	86	63	70	72
		2	119	80	58	103	90	86	64	71	72
	CU (%)	1	83	83	84	82	88	96	90	88	88
		2	82	83	84	81	88	96	90	88	88
	Drop diameter (mm)	Both	1.40	1.38	1.46	1.77	1.69	1.70	1.57	1.61	1.61
R4	Intensity (mmh^{-1})	1	139	95	71	126	111	103	85	93	87
		2	140	96	71	126	114	103	85	93	86
	CU (%)	1	88	81	87	92	93	94	91	90	85
		2	88	82	86	93	90	95	91	90	85
	Drop diameter (mm)	Both	1.47	1.46	1.44	1.84	1.60	1.72	1.59	1.59	1.62

3.4. Limitations of the Study and Future Research Directions

This research provides a holistic analysis of the spatial variability of I, CU, and D_{50} in one control plot simultaneously but has many limitations. All experiments were conducted in the climate-controlled chamber in the absence of wind conditions using one nozzle type and one installation height. Hence, the findings of the experiment may not be universally translated to larger simulators under wind conditions (Lasisi et al., 2022; Luza et al., 2024; Renner et al., 2024). Additionally, studies on the research specifically addressed the range of rainfall duration but have not specifically addressed the variability of intensity and drop size distribution in longer-duration rainfall despite the well-known effects of rainfall characteristics and variability in temporal scales in the generation of hydrological responses and erosivity (Henorman et al., 2022; Ma et al., 2023). The result presented variability based on the selected plot size and subplot design (A1 to A9); thus, a different spatial variability would have been experienced when a different configuration of the designs was considered. Indeed, the present outcome may serve as a controlled benchmark in the realization of the spatial variability in laboratory-scale rainfall simulators but may not present a general picture of all types of simulators. Future studies attempt to augment the present research further by incorporating the design approach for the consideration of all the rainfall characteristics in more intricate designs of simulators to realize more efficient KE distribution strategies (Fernández-Raga et al., 2022; Rončević et al., 2025; Renner et al., 2024).

4. Conclusion

Rainfall simulators are significant equipment in the sense that they enable the simulation of major events in the field of hydrology, including erosion, seepage, and drainage. Nevertheless, in order for the results to be correct and authentic, the simulation of the natural occurrence of rainfall needs to be very precise. The case in point clearly highlights the point that the spatial variation of parameters in the simulation of rainfall intensity, homogeneity, or droplet size significantly impacts the criteria of the efficiency of the rainfall simulator. The results show that assuming a single value for the *CU* across the entire channel area ignores significant regional differences. The findings clearly revealed that the variability in the intensity of the precipitation was more uniform in the middle portion of the channel. Additionally, the findings supported the point that the general trend of higher precipitation intensity resulted in more efficient uniformity. Despite the general trend being supported, the variation was also significant. The droplet size was not significantly correlated to the variation in the intensity of the rainfall.

These findings demonstrate that the application of individual values of the parameters of the performance in the whole research area can result in a loss of accuracy in the results of hydrological processes modeling in general, including the processes of soil erosion. This is particularly the case since the whole research area droplet size variability may influence the total amounts of soil transport. Including the whole research area in the analysis also provides a higher guarantee of a more accurate research approach. The research highlights the need for the development of a research approach to the designing of a calibration of the rainfall simulator.

A practical implication of these results would be that in experiments focused on infiltration, runoff, and erosion processes, one would need to restrict sampling or instrumentation to smaller sub-areas in which the values of *I*, *CU*, or D_{50} are known to vary less across the given site (e.g., the center of the plot) or account for the spatial variability of the rainfall input in designing the experiment. Failure to account for the spatial variability of the above factors would result in erroneous simulation of the rates of the processes under consideration in a rainfall simulator.

Acknowledgements

This study was presented as a poster at the EGU General Assembly 2025. The study was supported by the Scientific Research Projects Coordination Unit of Istanbul Technical University (ITU) (Project No: MYLB-2024-46054).

References

Abdollahi, Z. (2011). *Designing nozzles and testing rainfall characteristic in large soil erosion and sediment yield simulator* [M.Sc. thesis, Tarbiat Modares University].

Abudi, I., Carmi, G., & Berliner, P. (2012). Rainfall simulator for field runoff studies. *Journal of Hydrology*, *454*, 76–81. https://doi.org/10.1016/j.jhydrol.2012.05.056

Bentley, W. A. (1904). Studies of raindrops and raindrop phenomena. *Monthly Weather Review, 32,* 450–456.

Christiansen, J. E. (1941). The uniformity of application of water by sprinkler systems. *Agricultural Engineering, 22*(2), 89–92.

Clarke, M. A., & Walsh, R. P. D. (2007). A portable rainfall simulator for field assessment of splash and slopewash in remote locations. *Earth Surface Processes and Landforms, 32*(13), 2052–2069. https://doi.org/10.1002/esp.1593

Confesor, J. G., & Rodrigues, S. C. (2018). Método para calibração, validação e utilização de simuladores de chuvas aplicados a estudos hidrogeomorfológicos em parcelas de erosão. *Revista Brasileira de Geomorfologia, 19*(1), 25–38.

Demircioğlu, A. E., Kesgin, E., Gezici, K., & Şengül, S. (2024, 16–19 Ekim). *Farklı eğim koşullarına sahip yağış simülatörlerinde yağış şiddetinin alansal dağılımın incelenmesi* [Bildiri sunumu]. XII. Ulusal Hidroloji Kongresi, Samsun, Türkiye.

Fernández-Raga, M., Rodríguez, I., Caldevilla, P., Búrdalo, G., Ortiz, A., & Martínez-García, R. (2022). Optimization of a laboratory rainfall simulator to be representative of natural rainfall. *Water, 14*(23), Article 3831. https://doi.org/10.3390/w14233831

Fornis, R. L., Vermeulen, H. R., & Nieuwenhuis, J. D. (2005). Kinetic energy–rainfall intensity relationship for Central Cebu, Philippines for soil erosion studies. *Journal of Hydrology, 300,* 20–32. https://doi.org/10.1016/j.jhydrol.2004.04.027

Gezici, K., Kesgin, E., & Ağacıoğlu, H. (2021). Hydrological assessment of experimental behaviors for different drainage methods in sports fields. *Journal of Irrigation and Drainage Engineering, 147*(6), Article 04021034. https://doi.org/10.1061/(ASCE)IR.1943-4774.0001512

Gezici, K., Şengül, S., & Kesgin, E. (2025). Advances in sheet erosion and rainfall simulator performance: A comprehensive review. *Catena, 248,* Article 108601. https://doi.org/10.1016/j.catena.2025.108601

Green, D., & Pattison, I. (2022). Christiansen uniformity revisited: Re-thinking uniformity assessment in rainfall simulator studies. *Catena, 217,* Article 106424. https://doi.org/10.1016/j.catena.2022.106424

Henorman, V., Tholibon, A., Nujid, M., Mokhtar, M., Abd Rahim, E., & Saadon, S. (2022). The functional relationship of sediment transport under various simulated rainfall conditions. *Fluids, 7*(3), Article 107. https://doi.org/10.3390/fluids7030107

Iserloh, T., Fister, W., Seeger, M., Willger, H., & Ries, J. B. (2012). A small portable rainfall simulator for reproducible experiments on soil erosion. *Soil and Tillage Research, 124,* 131–137. https://doi.org/10.1016/j.still.2012.05.016

Kathiravelu, G., Lucke, T., & Nichols, P. (2016). Rain drop measurement techniques: A review. *Water, 8*(1), Article 29. https://doi.org/10.3390/w8010029

Kavian, A., Mohammadi, M., Cerda, A., Fallah, M., & Abdollahi, Z. (2018). Simulated raindrop's characteristic measurements: A new approach of image processing tested under laboratory rainfall simulation. *Catena, 167,* 190–197. https://doi.org/10.1016/j.catena.2018.04.034

Kesgin, E., Ağacıoğlu, H., & Doğan, A. (2020a). Experimental and numerical investigation of drainage mechanisms at sports fields under simulated rainfall. *Journal of Hydrology, 580,* Article 124251. https://doi.org/10.1016/j.jhydrol.2019.124251

Kesgin, E., Doğan, A., & Ağacıoğlu, H. (2018). Rainfall simulator for investigating sports field drainage processes. *Measurement, 125,* 360–370. https://doi.org/10.1016/j.measurement.2018.04.064

Kesgin, E., Gezici, K., & Ağacıoğlu, H. (2020b, 13–15 November). Hydrological evaluation of sports field drainage [Conference Paper] In *ISPEC 9th International Conference on Engineering & Natural Sciences* (pp. 182–191). Ankara, Turkey.

Kesgin, E., Gezici, K., & Ağacıoğlu, H. (2023). Spor sahaları drenajına genel bakış: Deneysel çalışma sistematiğinin oluşturulması. *Gazi Üniversitesi Mühendislik-Mimarlık Fakültesi Dergisi, 38*(4), 2495–2504. https://doi.org/10.17341/gazimmfd.1253839

Khaledian, H., & Shahoe, S. (2007, 21–23 August). *Assessment of raindrops size distribution to natural precipitation in Kurdistan Province, Iran* [Conference Paper]. Rainwater and Urban Design 2007*,* Sydney, Australia.

Koch, T., Chifflard, P., Aartsma, P., & Panten, K. (2024). A review of the characteristics of rainfall simulators in soil erosion research studies. *MethodsX, 12,* Article 102506. https://doi.org/10.1016/j.mex.2023.102506

Koşucu, M. E., Sarı, M., Demirel, M. C., Kıran, A., Yılmaz, G., Aybakan, Z., Albay, G. M., & Kırca, M. (2021). Gerçek zamanlı basınç yönetimiyle su dağıtım şebekesinde su kaybının azaltılması. *Teknik Dergi, 32*(2), 10541–10564.

Küçükerdem Öztürk, T. S., Saplıoğlu, K., & Güçlü, Y. S. (2025). Median ratio test on graphical representation for trend analysis by comparison with Mann–Kendall and Wilcoxon tests. *Hydrological Sciences Journal, 70*(14), 2530–2542. https://doi.org/10.1080/02626667.2025.2543943

Küçükerdem, T. S., Saplıoğlu, K., & Güçlü, Y. S. (2019). Bulanık çıkarım sistemlerinde kullanılan küme sayılarının K-ortalamalar ile belirlenmesi ve baraj hacmi modellenmesi: Kestel Barajı örneği. *Pamukkale Üniversitesi Mühendislik Bilimleri Dergisi, 25*(8), 962–967. https://doi.org/10.5505/pajes.2019.99223

Lasisi, K. H., Akinola, A. O., & Ogunjimi, L. A. O. (2022). Modification and performance evaluation of a small-scale rainfall simulator. *International Journal of Agriculture, Environment and Bioresearch, 7*(3), 273–285. https://doi.org/10.35410/IJAEB.2022.5736

Luk, S. H., Abrahams, A. D., & Parsons, A. J. (1993). Sediment sources and sediment transport by rill flow and interrill flow on a semi-arid piedmont slope, southern Arizona. *Catena, 20*(1–2), 93–111.

Luza, J. R., Almeida, W. S., Souza, A. G. S., Schultz, N., Anache, J. A. A., & Carvalho, D. F. (2024). Simulated rainfall in Brazil: An alternative for assessment of soil surface processes and an opportunity for technological development. *International Soil and Water Conservation Research, 12*(1), 29–42. https://doi.org/10.1016/j.iswcr.2023.05.002

Ma, Z., Liu, Y., Tian, X., Yang, J., Long, Y., Lei, T., Zhang, X., Li, Z., & Zhu, B. (2023). Effects of rainfall pattern and soil surface roughness on surface–subsurface hydrological response and particle size distribution of red soil slope. *Catena, 232*, Article 107422. https://doi.org/10.1016/j.catena.2023.107422

Meshesha, D. T., Tsunekawa, A., Tsubo, M., Haregeweyn, N., & Adgo, E. (2013). Drop size distribution and kinetic energy load of rainfall events in the highlands of the Central Rift Valley, Ethiopia. *Hydrological Sciences Journal, 59*(12), 2203–2215. https://doi.org/10.1080/02626667.2013.867371

Meshesha, D. T., Tsunekawa, A., Tsubo, M., Haregeweyn, N., & Tegegne, F. (2016). Evaluation of kinetic energy and erosivity potential of simulated rainfall using Laser Precipitation Monitor. *Catena, 137,* 237–243. https://doi.org/10.1016/j.catena.2015.09.017

Mhaske, S. N., Pathak, K., & Basak, A. (2019). A comprehensive design of rainfall simulator for the assessment of soil erosion in the laboratory. *Catena, 172,* 408–420. https://doi.org/10.1016/j.catena.2018.08.039

Moazed, H., Bavi, A., Boroomand-Nasab, S., Naseri, A., & Albaji, M. (2010). Effects of climatic and hydraulic parameters on water uniformity coefficient in solid set systems. *Journal of Applied Sciences, 10*(16), 1792–1796. https://doi.org/10.3923/jas.2010.1792.1796

Pérez-Latorre, F. J., de Castro, L., & Delgado, A. (2010). A comparison of two variable intensity rainfall simulators for runoff studies. *Soil and Tillage Research, 107*(1), 11–18. https://doi.org/10.1016/j.still.2010.01.006

Renner, C., Conroy, N., Thaler, E., Collins, A., Thomas, L., Dillard, S., Rowland, J., & Bennett, K. (2024). The next-generation ecosystem experiment arctic rainfall simulator: A tool to understand the effects of changing rainfall patterns in the Arctic. *Hydrology Research, 55*(1), 67–82. https://doi.org/10.2166/nh.2023.146

Rončević, T., Živanović, M., Radulović, M., Ristić, V., & Sadeghi, S. H. (2025). Design, calibration, and performance evaluation of a high-fidelity spraying rainfall simulator for soil erosion research. *Water, 17*(12), Article 1863. https://doi.org/10.3390/w17131863

Saplıoğlu, K., & Küçükerdem Öztürk, T. S. (2024). Effect of decision tree in the ANFIS models: An example of completing missing data. *Water Resources, 51*(5), 435–445.

Saplıoğlu, K., & Küçükerdem, T. S. (2018). Estimation of missing streamflow data using ANFIS models and determination of the number of datasets for ANFIS: The case of Yeşilırmak River. *Applied Ecology and Environmental Research*, *16*(3), 3583–3594. https://doi.org/ 10.15666/aeer/1603_35833594

Saplioglu, K., Kucukerdem, T. S., & Şenel, F. A. (2019). Determining rainwater harvesting storage capacity with particle swarm optimization. *Water Resources Management, 33*(14), 4749–4766. https://doi.org/10.1007/s11269-019-02389-3

Şenel, F. A., Öztürk, T. S. K., & Saplıoğlu, K. (2020). Yeşilırmak nehri akış verisi tahmininin yapay sinir ağları kullanılarak karınca aslanı algoritması ile zaman gecikmesi boyutunun optimizasyonu. *Afyon Kocatepe Üniversitesi Fen ve Mühendislik Bilimleri Dergisi, 20*(2), 310–318. https://doi.org/10.35414/akufemubid.669602

Sousa, S. F. D., Mendes, T. A., & Siqueira, E. Q. D. (2017). Development and calibration of a rainfall simulator for hydrological studies. *Revista Brasileira de Recursos Hídricos, 22,* Article e59. https://doi.org/10.1590/2318-0331.011716018

Tan Kesgin, R. İ. (2025). Revisiting trend stability using Mann-Kendall and Wilcoxon Signed-Rank tests through innovative method comparisons. *Sustainability, 17*(23), Article 10454. https://doi.org/10.3390/su172310454

Van Dijk, A. I. J. M., Bruijnzeel, L. A., & Rosewell, C. J. (2002). Rainfall intensity–kinetic energy relationships: A critical literature appraisal. *Journal of Hydrology, 261*(1–4), 1–23. https://doi.org/10.1016/S0022-1694(01)00511-8

Zhang, X., Yu, G. Q., Li, Z. B., & Li, P. (2014). Experimental study on slope runoff, erosion and sediment under different vegetation types. *Water Resources Management, 28*(8), 2415–2433. https://doi.org/10.1007/s11269-014-0603-5